Protein Science (1993), *2*, 2206–2216. Cambridge University Press. Printed in the USA.

Thermal stability and conformational transitions of scrapie amyloid (prion) protein correlate with infectivity

JIRI SAFAR,[1] PETER P. ROLLER,[2] D. CARLETON GAJDUSEK,[1] AND CLARENCE J. GIBBS, JR.[1]

[1] Laboratory of Central Nervous System Studies, National Institute of Neurological Disorders and Stroke, and
[2] Laboratory of Medicinal Chemistry, DTP, DCT, National Cancer Institute, National Institutes of Health, Bethesda, Maryland 20892

(RECEIVED June 24, 1993; ACCEPTED September 7, 1993)

Abstract

The scrapie amyloid (prion) protein (PrP27-30) is the protease-resistant core of a larger precursor (PrP^{Sc}) and a component of the infectious scrapie agent; the potential to form amyloid is a result of a posttranslational event or conformational abnormality. The conformation, heat stability, and solvent-induced conformational transitions of PrP27-30 were studied in the solid state in films by CD spectroscopy and correlated with the infectivity of rehydrated and equilibrated films. The exposure of PrP27-30 in films to 60 °C, 100 °C, and 132 °C for 30 min did not change the β-sheet secondary structure; the infectivity slightly diminished at 132 °C and correlated with a decreased solubility of PrP27-30 in sodium dodecyl sulfate (SDS), probably due to cross-linking. Exposing PrP27-30 films to formic acid (FA), trifluoroacetic acid (TFA), trifluoroethanol (TFE), hexafluoro-2-propanol (HFIP), and SDS transformed the amide CD band, diminished the mean residue ellipticity of aromatic bands, and inactivated scrapie infectivity. The convex constraint algorithm (CAA) deconvolution of the CD spectra of the solvent-exposed and rehydrated solid state PrP27-30 identified five common spectral components. The loss of infectivity quantitatively correlated with a decreasing proportion of native, β-pleated sheet-like secondary structure component, an increasing amount of α-helical component, and an increasingly disordered tertiary structure. The results demonstrate the unusual thermal stability of the β-sheet secondary structure of PrP27-30 protein in the solid state. The conformational perturbations of PrP27-30 parallel the changes in infectivity and suggest that the β-sheet structure plays a key role in the physical stability of scrapie amyloid and in the ability to propagate and replicate scrapie.

Keywords: conformation; infectivity; prion protein; scrapie amyloid; transitions

Recent molecular biological and genetic evidence demonstrates that the abnormal isoform of the host cell-derived scrapie amyloid (prion) protein plays a central role in the development of spongiform encephalopathies (Gajdusek, 1988; Prusiner, 1992). The scrapie amyloid (prion) protein, a critical factor involved in neuronal degeneration, undergoes a three-stage transition during disease development: normal form of scrapie amyloid precursor (cellular isoform of prion protein, PrP^{C}) → infectious form (scrapie isoform of prion protein, PrP^{Sc}) → scrapie amyloid (prion protein, PrP27-30) (Gajdusek, 1988; Prusiner, 1992). Such a cascade occurs not only in scrapie in sheep and goat, but also during the development of encephalopathy in mink, chronic wasting disease in deer and elk, bovine spongiform encephalopathy in cattle, and Creutzfeldt-Jakob disease (CJD), kuru, Gerstmann-Straussler-Sheinker syndrome (GSS), and fatal familial insomnia in man (Gajdusek, 1988; Prusiner, 1992).

Because both PrP^{C} and $PrP^{Sc/CJD}$ protein isoforms are encoded by the same cellular gene, and because until now chemical differences between them have not been

Reprint requests to: Jiri Safar, Laboratory of Central Nervous System Studies, National Institute of Neurological Disorders and Stroke, NIH, Building 36, Room 4A-15, Bethesda, Maryland 20892.

Abbreviations: CCA, convex constraint analysis; FA, formic acid; HFIP, 1,1,1,3,3,3-hexafluoro-2-propanol (hexafluoroisopropanol); HPLC, high-performance liquid chromatography; PAGE, polyacrylamide gel electrophoresis; PBS, phosphate-buffered saline; PMSF, phenylmethyl sulfonyl fluoride; $PrP^{Sc/CJD}$, scrapie (Sc) or Creutzfeldt-Jakob disease (CJD) isoform of prion protein; PrP^{C}, normal isoform of prion protein; PrP27-30, prion protein; SDS, sodium dodecyl sulfate; TBS, 10 mM Tris, 100 mM NaCl; TEM, transmission electron microscopy; TFA, trifluoroacetic acid; TFE, 2,2,2-trifluoroethanol; [θ], mean residue ellipticity.

observed (Prusiner, 1992), it is possible that both amyloid formation and disease transmission result from conformational transitions in the PrP molecule. Such a conformational transition may be facilitated either by point mutations, interactions with a theoretically proposed ligand (Weissmann, 1991), or yet undetected posttranslational events. Recent IR spectroscopy studies (Caughey et al., 1991; Gasset et al., 1993) confirmed a high content of β-sheets in the secondary structure of PrP27-30, as had been anticipated from the TEM appearance and green birefringence of Congo red-stained scrapie amyloid fibrils (SAFs) or prion rods (Prusiner et al., 1983). However, the secondary and tertiary structure of full-length PrP^{Sc}, the secondary and tertiary structure of PrP^{C}, and the molecular mechanism of the transitions of PrP^{C} to PrP^{Sc} are not known. Another characteristic of the scrapie agent is the extreme resistance to heat and physical inactivation (Brown et al., 1990a), which has never been fully explained. It is critical to understand the relationship between the conformation of PrP27-30 and the ability to propagate, replicate, and cause disease.

Previously, we have shown that proteins and peptides aggregate on glass and mica surfaces in amorphous, glass-like films with preserved secondary structures (Safar et al., 1993). In this paper, we have used CD spectroscopy of the PrP27-30 protein in the solid state and explored the phenomenon that the change in the secondary structure of the protein induced by organic solvent remained stable in the solid state after rapid solvent elimination (Safar et al., 1993). The resulting films, rehydrated and equilibrated in H_2O, and displaying stable CD spectra, were assayed for infectivity in hamsters. The results indicate that the native β-sheet secondary structure of PrP27-30 remains stable in the solid state after exposure to 132 °C for 30 min, and that the minor decrease in infectivity after exposure parallels the cross-linking of PrP27-30 with resulting lower solubility. In contrast, the chemical scrapie inactivators such as FA, SDS, additional α-helix-inducing fluorinated alcohols, and TFA had dramatic effects on the secondary and tertiary structure of PrP27-30 in the solid state and on the infectivity. Secondary structure analysis by the CCA algorithm indicates that loss of the native β-pleated sheet-like secondary and tertiary structure correlates with inactivation of scrapie infectivity.

Results

Purification, bioassay, and CD spectroscopy of PrP27-30 films

As estimated from the densitometry of silver-stained gels (Fig. 1), the purity of PrP27-30 after proteinase K cleavage was ≥95%. The triplet bands on silver-stained gels and Western blots reflect different levels of glycosylation (Safar et al., 1990). Reconstituting the PrP27-30 film by sonication in H_2O recovered most of the infectivity (Table 1), when compared with the sonicated original suspension in H_2O.

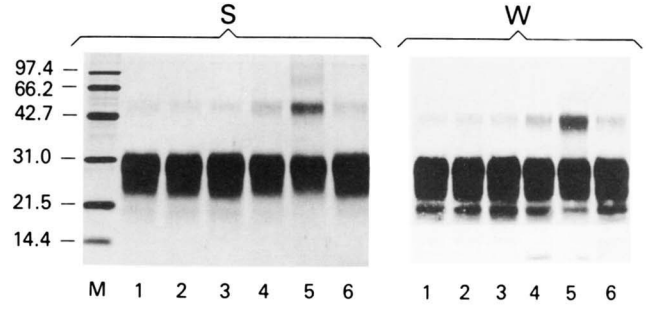

Fig. 1. Effect of heat and formic acid on PrP27-30 in the solid state. The films of PrP27-30 made on glass were exposed for 30 min to different temperatures, reconstituted into original volume in H_2O, boiled for 5 min in Laemmli buffer, separated on 12.5% SDS-polyacrylamide gels, and detected by silver staining (S) or Western blots (W). Sample 1, original suspension of PrP27-30 in PBS, pH 7.2; sample 2, film of PrP27-30 exposed to 23 °C; sample 3, film exposed for 30 min to 60 °C; sample 4, exposed for 30 min to 100 °C; sample 5, exposed for 30 min to 132 °C; sample 6, films of PrP27-30 exposed for 30 min to FA, dried by Speed-Vac, kept under vacuum in a desiccator for 24 h above KOH pellets, and then reconstituted in H_2O and boiled in Laemmli buffer. M_r of the marker is in kDa.

The near-UV CD spectra of dry PrP27-30 films showed a broad low-intensity aromatic positive band centered at 261 nm with a negative component at 290 nm (Figs. 2, 4). The symmetric negative band in the amide region has a minimum at 222.5 nm, crossover at 206 nm, and weak

Table 1. *Cumulative data on the effect of heat and solvents on scrapie infectivity in PrP27-30 samples as measured by incubation time assay*[a]

Sample	Exp. (*n*)	Infectivity ± SEM (log ID_{50}/mL)
PrP27-30 susp/PBS	3	9.4 ± 0.2
PrP27-30 film/23 °C	3	8.9 ± 0.3
PrP27-30 film/60 °C	2	8.8 ± 0.5
PrP27-30 film/100 °C	2	8.7 ± 0.3
PrP27-30 film/132 °C	2	7.6 ± 0.1
PrP27-30 film/SDS	3	6.8 ± 0.2
PrP27-30 film/TFE	1	7.9 ± 0.4[b]
PrP27-30 film/HFIP	4	7.1 ± 0.1
PrP27-30 film/TFA	1	<2
PrP27-30 film/FA	5	<2

[a] PrP27-30 susp/PBS, purified protein resuspended in PBS, pH 7.4; PrP27-30 film, the films cast from H_2O and exposed for 30 min to: 23 °C, 60 °C, 100 °C, 132 °C, SDS (270× molar excess), TFE, HFIP, TFA, and 99% FA. All films were rapidly dried in a Speed-Vac, stored for ≥24 h at 23 °C in a vacuum above KOH pellets, rehydrated with H_2O for 24 h, and reconstituted by 15 min sonication in a sonication bath in PBS, pH 7.4. The titer is an average ± SEM calculated from n experiments; each sample titrated at dilution of 10^{-2} or 10^{-3} on eight golden Syrian hamsters.

[b] SEM is the standard error of one bioassay on eight animals.

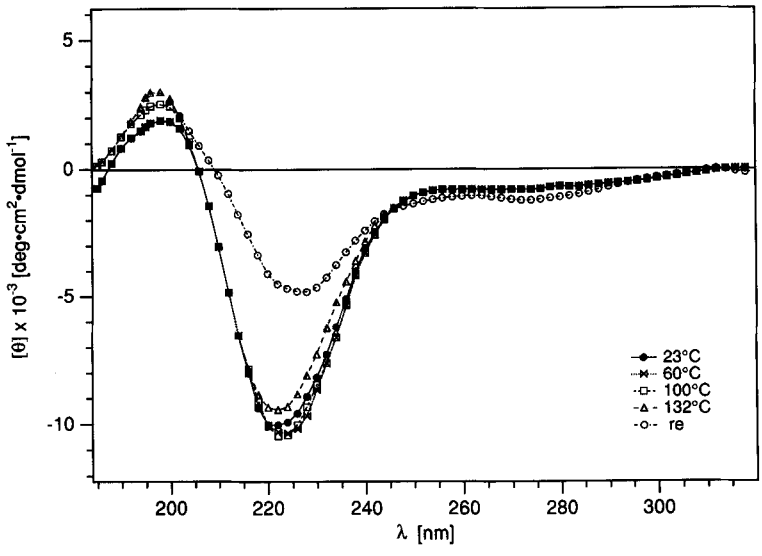

Fig. 2. Thermal stability of PrP27-30 conformation in the solid state. The films of PrP27-30 were cast from 100 μL of 9 μM solution in H_2O, exposed for 30 min to 23 °C, 60 °C, 100 °C, or 132 °C, and the UV CD spectra were recorded at 23 °C; "re" is the CD spectrum of the film first exposed to 132 °C, rehydrated at 23 °C for 24 h in H_2O, and then recorded.

positive component toward 197 nm (Figs. 2, 4). Rehydration of the films decreased molar ellipticity and red-shifted both CD bands: the aromatic band to 263.5 nm and the amide to 226–227 nm (Figs. 2, 4). There were no changes in the spectra after 30 min of rehydration.

High-temperature effect on PrP27-30 in solid state

The temperature measured directly inside the vessels containing protein films reached equilibrium at 132 °C within 11 min, and cooling back to 23 °C was achieved in a comparable time period (data not shown). The dry films exposed to different temperatures were reconstituted in Laemmli sample buffer, boiled for 5 min at 100 °C, and run on 12.5% PAGE in the presence of 0.1% SDS (Fig. 1). The pattern of PrP27-30 protein reconstituted from films exposed to 23 or 60 °C showed neither qualitative nor quantitative changes when compared to the original PrP27-30 solution. There was increased intensity of dimer and higher oligomer bands in the gels after exposure to 100 °C, and more at 132 °C with a parallel decrease in the proportion of monomers (Fig. 1). The densitometry of the sample after exposure to 132 °C (not shown) indicated a decrease in the total amount of PrP27-30 to 40% of the original and an increase of dimers and higher oligomers from 7 to 14%.

The CD spectrum recorded at 23 °C after exposure of the protein for 30 min to different temperatures showed no changes in the band maxima and crossover points, with less than ~5% decrease in ellipticity amplitude at 132 °C from that of the original film (Fig. 2). The CD spectrum of the film rehydrated after exposure to 132 °C decreased the ellipticity, red-shifted the amide band minimum by 5 nm, and increased the ellipticity of both the 260-nm aromatic peak and its negative component at 290 nm (Fig. 2). There was no difference between hydrated heated and nonheated films.

The infectivity of dried, heated, and then reconstituted PrP27-30 films assayed on two PrP27-30 samples (Fig. 3) underwent only minor changes while exposed for 30 min to different temperatures. After exposure to 132 °C, the decrease in infectivity was 0.6 and 1.3 log ID_{50}/mL, respectively, compared to the original untreated films. Only the difference of 1.3 log ID_{50}/mL was statistically significant (ANOVA; $P < 0.05$).

Solvent exchange effect on conformation and infectivity of PrP27-30

The amide CD spectra of PrP27-30 films treated with SDS and different organic solvents (Fig. 4) revealed a uniform response: the appearance of a double negative band

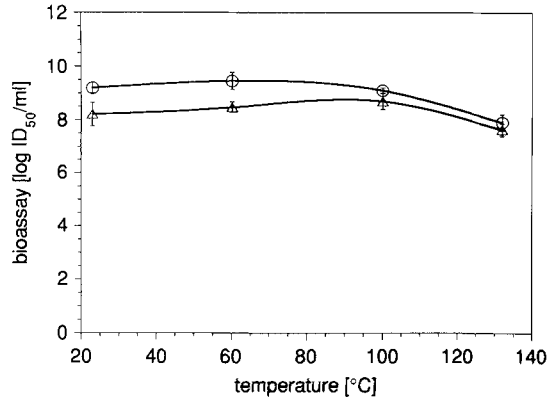

Fig. 3. Thermal resistance of the infectivity of PrP27-30 samples in the solid state. The films of PrP27-30 were cast from 100 μL of 9 μM solution in H_2O, exposed for 30 min to 23 °C, 60 °C, 100 °C, or 132 °C, rehydrated at 23 °C for 24 h in H_2O, sonicated for 15 min in a sonication bath, and assayed for infectivity. Plots are the results of two independent experiments. Bars are the SEM of the incubation time assay on eight animals.

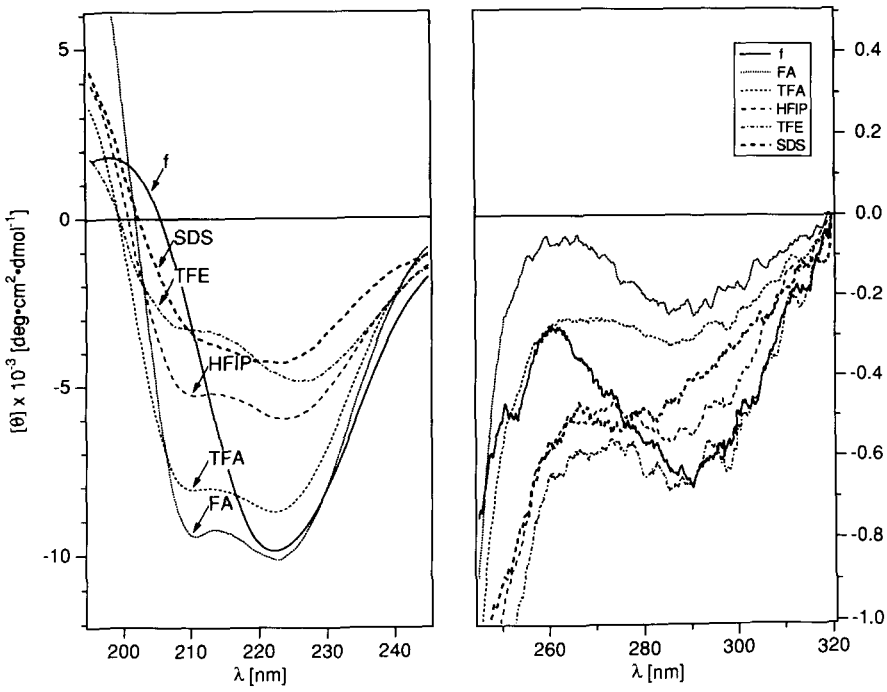

Fig. 4. Solvent-induced conformational transitions of PrP27-30 in the solid state in films on quartz glass. The far-UV (left) and near-UV (right) CD spectra of the PrP27-30 film cast from 100 μL of 9 μM solution in H_2O at 23 °C. f, UV CD spectrum of PrP27-30 film recorded at 23 °C, no treatment; SDS, film exposed for 30 min to 270× molar excess of SDS (SDS/protein molar ratio); TFE, film exposed for 30 min to trifluoroethanol; HFIP, film exposed for 30 min to hexafluoroisopropanol; TFA, film exposed for 30 min to trifluoroacetic acid; FA, film exposed for 30 min to 99% formic acid. All films were stored ≥24 h at 23 °C in a vacuum above KOH pellets before recording.

at ~208–210 and 222–226 nm and a positive band toward ~195 nm. The negative $[\theta]$ at 208 nm progressively increased from PrP27-30 films cast from water in the following order: water → TFE → SDS → HFIP → TFA → FA-treated films. The crossover point blue-shifted from 206 nm in the native film to 200 nm in TFA- and FA-treated films. The aromatic spectrum underwent complex perturbations, showing different effects in the various solvents, but with generally decreasing $[\theta]$ at 290 nm in the following order: native → TFE → HFIP → SDS → TFA → FA-treated films (Fig. 4). The results of CD spectroscopy of the films cast directly from PrP27-30 solutions in the above solvents were identical.

The CD spectra of rehydrated films that were treated with SDS or organic solvents or cast from proteins dissolved in organic solvents (Fig. 5), exhibited decreased

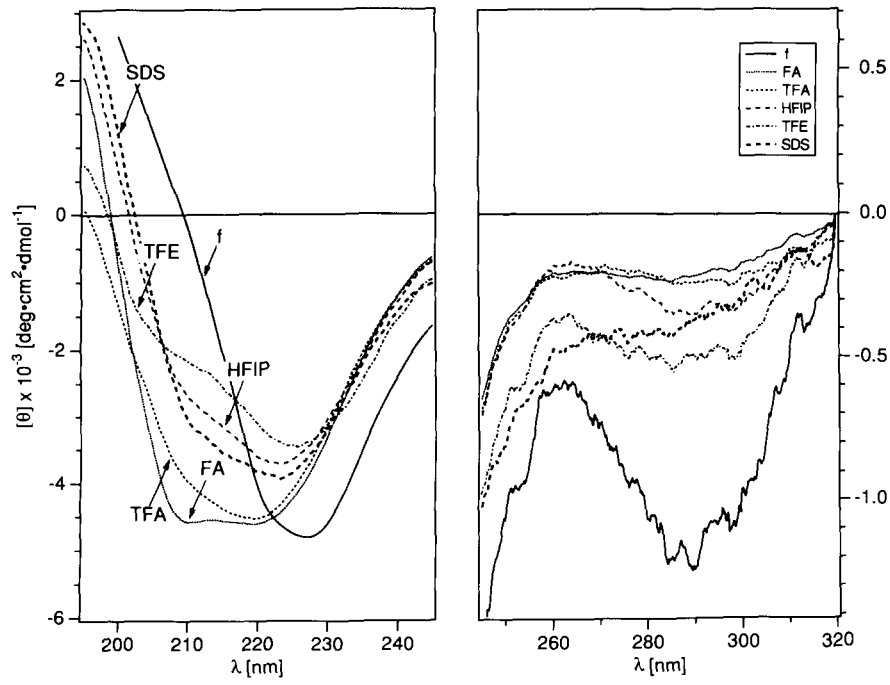

Fig. 5. Effect of hydration on solvent-induced conformational transitions of PrP27-30 in the solid state. The far-UV (left) and near-UV (right) CD spectra of the PrP27-30 films treated as in previous experiments (Fig. 4), rehydrated for 24 h in H_2O (see Materials and methods), and recorded at 23 °C. f, UV CD spectrum of the rehydrated PrP27-30 film at 23 °C, no treatment; SDS, rehydrated SDS-treated film; TFE, rehydrated trifluoroethanol-exposed film; HFIP, rehydrated hexafluoroisopropanol-exposed film; TFA, rehydrated trifluoroacetic acid-exposed film; FA, rehydrated formic acid-exposed film.

amplitude of negative [θ] comparable to that seen in the native film. The spectra had general characteristics similar to both the rehydrated native and the dry, organic solvent-treated films. The amide double-negative band remained but the amplitude ratio at 208 and 222 nm decreased. Additionally, with decreasing amplitude of ellipticity at 208 nm, there was a progressive shift of the second band to a higher wavelength: from 220 nm of FA-treated film to 225 nm of TFE-treated and 227 nm of untreated film. The aromatic spectra showed complex perturbations of the bands with generally decreased [θ] in rehydrated, solvent-treated films versus nontreated films (Fig. 5). The aromatic spectral regions of FA- and TFA-treated films were flat and close to the baseline; there was a trend toward lower CD band amplitudes at 290 nm in the following order: native → TFE → SDS → HFIP → TFA → FA-treated films. The CD spectra of organic solvent-treated films changed within the first minutes of rehydration, and after 30 min remained stable for 24 h.

The results of the bioassay of the solvent-treated and rehydrated films in hamsters, summarized in Table 1, showed different levels of infectivity after each organic solvent replacement. The results of FA- and TFA-treated films are expressed as <2 log ID_{50}/mL, indicating that the result is less than the sensitivity limit of the bioassay.

Deconvolution of PrP27-30 by CCA algorithm

The deconvolution of the 12 CD spectra of PrP27-30 in the solid state into an increasing number of components gave the deflection point at $P = 5$; further increase in the number of components did not significantly increase the accuracy of deconvolution (Fig. 6). The "pure" component spectra for the increasing number of components are in Figure 7. None of the deconvolution up to 10 components gave the solution-like "random coil" spectra (Woody, 1985), and all of them, starting from $P = 3$ deconvolution, maintained the spectrum corresponding to the dry film of PrP27-30 as a "pure" component (Fig. 7). The observed CD spectrum of HFIP-exposed rehydrated PrP27-30 film and the spectrum that had been calculated from conformational weights and five "pure" spectral components are very similar (Fig. 8).

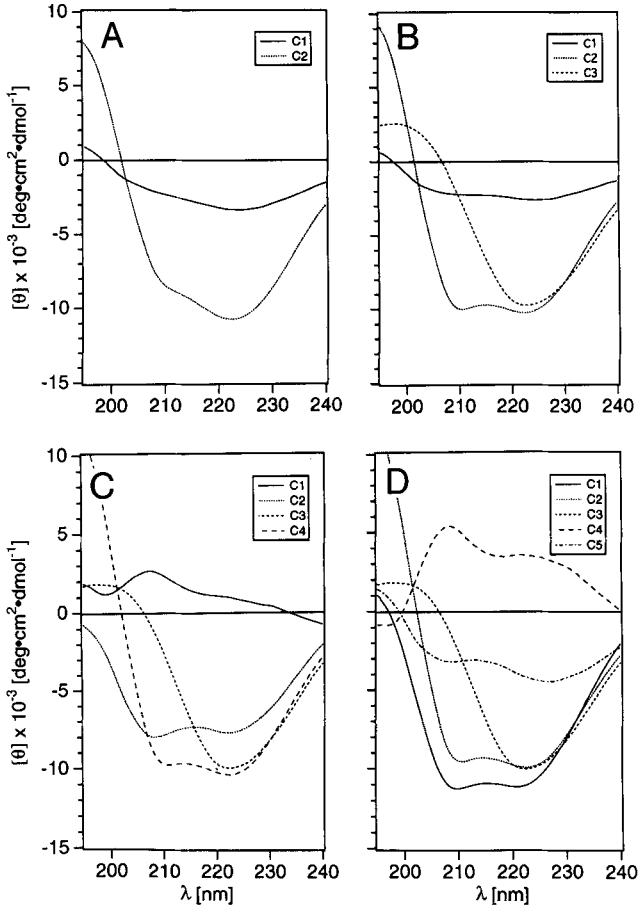

Fig. 7. "Pure" component curves obtained by CCA analysis from PrP27-30 solvent exchange database for two- (**A**), three- (**B**), four- (**C**), and five- (**D**) component deconvolutions. The assignments for a five-component deconvolution (D, $P = 5$) are: C1, β-turn type I(III), or 3_{10}-helix-like component; C2, α-helix-type component; C3, native β-pleated-sheet-like component; C4, β-turn type II component; C5 component, additional chiral contribution.

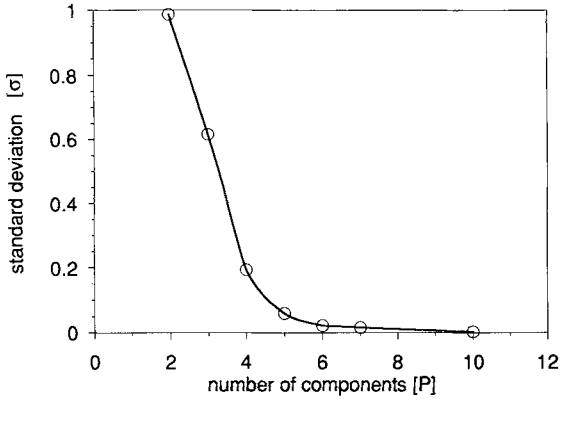

Fig. 6. Dependency of the standard deviation (σ) of the CCA deconvolution on the number of components (P) obtained for the set of 12 solid state PrP27-30 CD spectra from solvent exchange experiments (Figs. 4, 5).

Relationship of secondary structure perturbation and infectivity

The results of the CCA method were used to estimate the changes in spectral contribution (Table 2) of the native β-pleated sheet-like component (C3) to PrP27-30 CD spectra from solvent replacement studies. The plot (Fig. 9) indicates a correlation between the percentage of native β-pleated sheet-like spectral component (C3) and infec-

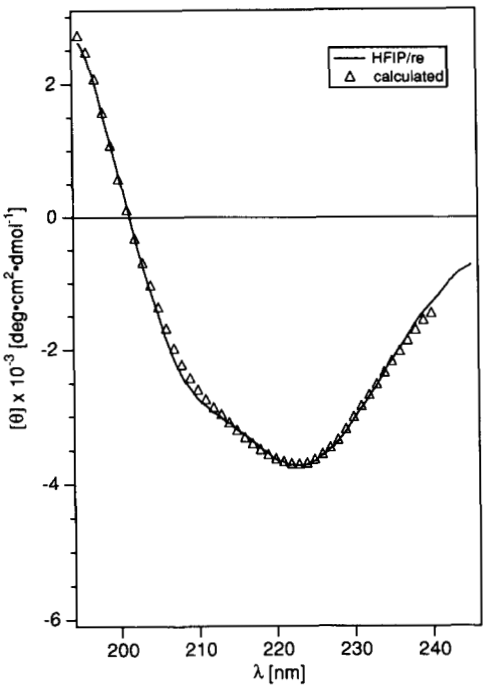

Fig. 8. CD curve of HFIP-treated, rehydrated PrP27-30 film as measured (line) and calculated (triangles) as the best fit by CCA analysis.

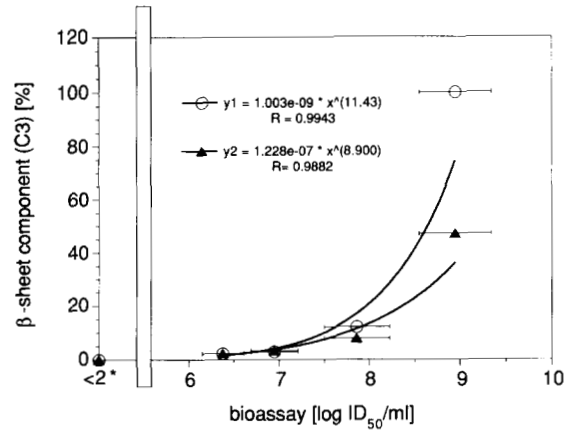

Fig. 9. Correlation of the solvent-induced changes in the native β-pleated-sheet-like spectral component of PrP27-30 and infectivity. The plots are the least-square fits of spectral weights of the β-pleated-sheet-like component (C3) obtained by CCA analysis (Perczel et al., 1991b) for solvent-treated PrP27-30 films (Figs. 4, 5) and infectivity. The data for dehydrated films are indicated by open circles, for rehydrated films by triangles. The data on FA- and TFA-treated films (*) are expressed as a range; they were excluded from the least-square fit. The bars are the SEM of the bioassay.

tivity for both dry and rehydrated organic solvent-treated films. In contrast, the spectral weight of the α-helix-like component (C2) was inversely proportionate to infectivity (Fig. 10). The statistics did not incorporate the results of the infectivity bioassay of TFA- and FA-treated samples because the results were below the sensitivity limit of the bioassay.

Table 2. *The perturbation effect of solvents on the CD spectra of dry (C1-5) and rehydrated (C1re-5re) hamster PrP27-30 protein in the solid state at 23 °C*[a]

	C1	C1re	C2	C2re	C3	C3re	C4	C4re	C5	C5re
f23	0.0	0.0	0.0	0.0	99.8	47.1	0.1	52.9	0.1	0.0
TFE	0.0	13.6	9.9	3.2	12.1	7.9	0.1	16.9	77.9	58.4
HFIP	11.2	17.0	31.7	21.7	3.0	3.3	6.9	40.0	47.2	18.0
SDS	13.3	13.3	35.4	37.1	2.7	2.3	39.0	39.4	9.6	7.9
TFA	22.1	34.9	73.4	50.0	0.0	0.0	0.1	15.0	4.4	0.1
FA	20.6	23.1	79.3	68.4	0.0	0.0	0.0	1.3	0.1	7.2

[a] The native film of PrP27-30 at 23 °C is labeled f23; the rest of the labels indicate the solvent used for the conformational perturbations. The spectral component weights were obtained by the deconvolution of the set of 12 PrP27-30 CD spectra by the CCA program (Perczel et al., 1991b) into five common ($P = 5$) components: C1, β-turn type I(III), or 3_{10}-helix-like component; C2, α-helix-type component; C3, native β-pleated-sheet-like component; C4, β-turn type II component; C5 component, additional chiral contribution. The contribution of each component to the final spectra is expressed as percent of the total.

Discussion

When the proteins in solid state are exposed to (or cast from) organic solvents, they retain the solvent-induced secondary structure after elimination of the solvent in a vacuum (solvent "memory" effect) (Stevens, 1977; Safar et al., 1993). This finding and the fact that the PrP27-30 reconstituted from dry films is infectious were used in this

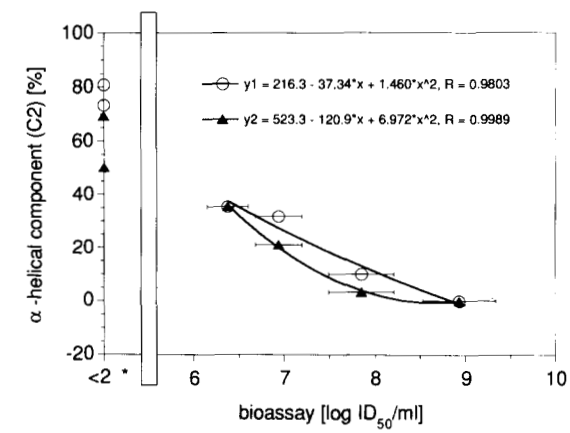

Fig. 10. Inverse correlation of the solvent-induced α-helix-like spectral component of CD spectra of PrP27-30 and infectivity. The plots are the least-square fits of spectral weights of the α-helix-like (C2) component obtained by CCA analysis (Perczel et al., 1991b) for solvent-treated PrP27-30 films and infectivity. The data for dehydrated films are indicated by open circles, for rehydrated films by triangles. The data for FA- and TFA-treated films (*) are expressed as a range; they were excluded from the least-squares fit. Bars are the SEM of the incubation time assay.

paper to determine the conformational impact of the hydration, heat, and organic solvents on PrP27-30 in the solid state and to correlate the resulting conformational changes with the infectivity of rehydrated, equilibrated, and conformationally stable films.

Both CD spectra of dry and hydrated PrP27-30 can be assigned to type II-β spectra (Stevens et al., 1968; Woody, 1985) with the $n\pi^*$ transition red-shifted to 222.5 nm in dry and 227 nm in rehydrated films. The higher amplitude of the aromatic bands in the CD spectra of the hydrated film indicates that the shift of the amide band is at least partially due to the strong aromatic coupling (Stevens et al., 1968; Auer, 1973). An additional contribution may come from a different β-sheet twist in the dry and hydrated states (Woody, 1985). The loss of free water in the solid state apparently increased (Greenfield & Fasman, 1969) the β-sheet content in the PrP27-30 secondary structure, altered the tertiary structure (Ewbank & Creighton, 1991) of PrP27-30 into a less ordered one, but did not change the infectivity. The β-sheet growth in the dry state is probably due to the intermolecular alignment of external β-sheets, or to the intramolecular secondary structure transition favoring β-sheets, or both. The observed changes may simulate the PrP27-30 conformational transitions in amyloid plaques upon early aggregation of PrP27-30 in the extracellular space.

An important characteristic of agents causing spongiform encephalopathies (prion disease) is their exceptional thermal resistance (Rohwer, 1984; Brown et al., 1990a). Although most of the inactivation experiments were performed with whole tissue or crude homogenates (for review, see Asher et al. [1986]), it appears that a portion of scrapie and CJD infectivity is heat resistant, under some circumstances for $\geq$60 min at 132 °C (Brown et al., 1990a). This is difficult to explain by any hypothesis, and in the case of the "protein only" prion model (Prusiner, 1992), it implies reversibility of the protein thermal unfolding or a very unusual conformational heat resistance (Creighton, 1990). However, all proteins from the scrapie host organisms undergo full unfolding (denaturation) between 40 and 80 °C; the process is irreversible if the proteins aggregate (Jaenicke, 1987).

The experiments with purified PrP27-30 in dehydrated thin films exposed to heat for 30 min indicated no change of infectivity at 100 °C and a minor drop at 132 °C. At the same time, the secondary structure of this protein was heat-resistant in the solid state and there were no significant changes after exposure to 132 °C. The slightly diminished infectivity at 132 °C correlated with less PrP27-30 protein entering the SDS-polyacrylamide gel, and with an increased percentage of dimers and higher oligomers. The most likely explanation is the side-chain cross-linking at high temperature (Jaenicke & Rudolph, 1986). The secondary structure of PrP27-30 in the solid state apparently has the necessary thermal stability to be a carrier of infectivity. Our recent data on some model proteins and peptides indicate that this heat stability of the β-sheet structured protein in the solid state is not exceptional (Safar et al., 1993) and may be explained by the absence of free solvent (Schulz & Schirmer, 1979).

Solvent perturbation studies of the PrP27-30 secondary structure in the solid state followed by CD spectroscopy indicate loss of native β-pleated sheet-like secondary and tertiary structure after FA, TFA, fluorinated alcohols, or after SDS treatment. Equivalent results were obtained with the films cast directly from FA, TFA, or SDS solutions. When the films were rehydrated, the resulting CD spectrum showed a combination of the characteristics of dry, solvent-treated, and native-rehydrated film. None of the CD spectra of the rehydrated and solvent-treated proteins indicated a full return to a nativelike secondary or tertiary structure within 48 h. The strongest α-helix inducer was FA, which is known to inactivate scrapie infectivity (Brown et al., 1990b). The structural effect of FA may be explained by the formation of temporary hydrogen bonds in the protein. During FA evaporation and in the absence of water, the FA hydrogen bonds are replaced by intrachain (α-helix) or interchain (β-sheet) hydrogen bonds in a zipperlike manner (Nakajima et al., 1973; Kugo et al., 1992; Safar et al., 1993). Simultaneously, the PrP27-30 film loses infectivity. The TFA and fluorinated alcohols, TFE and HFIP, are also H-bond donors and α-helix- or β-turn-promoting solvents (Barrow et al., 1992; Hollosi et al., 1992); they induced a different degree of β-to-α secondary and tertiary structure transitions of PrP27-30 and proportionally diminished the residual infectivity of the film. Despite its hydrophobic interactions, SDS is also an α-helix inducer at the molar ratio SDS/protein >270:1 (Safar et al., 1993), and at the same time, SDS decreases the infectivity of PrP27-30 (this paper and Safar et al. [1990]). The lack of recovery of infectivity from FA- and TFA-treated films and the recent study of the effect of SDS, GdnSCN, and urea on the infectivity of PrP27-30 (Prusiner et al., 1993) indicate irreversible inactivation with no reactivation in vitro or in vivo.

In order to decipher the solvent perturbation effects on the secondary structure of dry and hydrated PrP27-30 proteins, we deconvoluted the set of the PrP27-30 CD spectra with the recently introduced CCA method (Perczel et al., 1991b). Neither fixed nor variable reference methods, commonly used for quantitative protein CD spectra deconvolution, could be applied to the solid state for the following reasons: (1) the variable differences in $[\theta]$ in the dry and fully hydrated state (this paper and Safar et al. [1993]); (2) all reference databases are based on solution spectra (Woody, 1985; Yang et al., 1986); and (3) the apparently different (or nonexistent) solution-derived "random coil" or "open" CD spectrum in solid state (Safar et al., 1993). In order to overcome the bias effect of the database composition, the CCA algorithm operates to extract the common components based on the number

of components (P) as an input parameter (Perczel et al., 1991b). The natural deconvolution by CCA algorithm has already been applied to measure conformational weights and extract pure components from the CD spectra sets of globular (Perczel et al., 1991b; Park et al., 1993) or membrane proteins (Park et al., 1992); to analyze the conformational transitions of linear polypeptides during ion titration (Hollosi et al., 1992); and to investigate the CD spectrum and conformational interconversion of β-turn model peptides (Perczel et al., 1991a; Perczel & Fasman, 1992).

The statistically satisfactory (Perczel et al., 1991b; Park et al., 1992) deconvolution of the set of PrP27-30 CD spectra (Figs. 4, 5) was obtained with five ($P = 5$) components. The first "pure" component (C1) resembles the class C spectrum (Woody, 1985), and by the blue-shifted crossover point and the low intensity positive band of $\pi\pi^*$ transition may correspond to that of a type I(III) turn (Perczel & Fasman, 1992) or 3_{10}-helix (Miick et al., 1992). The second component (C2) has all the characteristics of an α-helix (Woody, 1985); the third component (C3) was assigned to the red-shifted β-sheet (II-β) (Stevens et al., 1968; Woody, 1985); and the fourth (C4) component closely resembles the class C′ spectrum and could indicate spectra of type II β-turn or similar structure (Woody, 1985; Perczel & Fasman, 1992). The fifth component (C5) is an additional chiral contribution and may indicate the presence of another secondary structure element, or the contribution of disulfidic and aromatic residues (Brahms & Brahms, 1980; Perczel et al., 1991b). The amplitude of a "pure" α-helix-like spectral component is lower then expected. Whether or not it is the α-helical end-effect or a different amplitude of CD spectra of this secondary structure element in the solid state is not clear. For that reason, the spectral weights obtained from CCA deconvolution should not be taken as conformational weights of secondary-structure elements until the relationship is verified by a large enough solid-state database or by an independent technique. The striking observation is that no deconvolution of PrP27-30 CD spectra in solid state led to a solution-like "random coil" or "open" spectral component. The absence of solution-like "random coil" CD spectra in the solid state was previously suggested by parallel solid state CD and IR studies of proteins and model peptides (Safar et al., 1993). Additionally, the persistence of II-β-sheet-type spectra through the deconvolution process indicates unique spectral properties (Woody, 1985).

The correlation of spectral weights of each "pure" component with infectivity confirmed that all the solvents used in this study decreased the percentage of the native β-sheets, increased the amount of secondary structure in an α-helix-like conformation, and simultaneously diminished infectivity. Analogous results were obtained by calculating the percentage of the α-helical secondary structure from $[\theta]$ at 208 nm (Greenfield & Fasman, 1969) or correlating the CD fractional changes at 208 nm (Matthews & Crisanti, 1981) with infectivity (data not shown). The concurrent perturbations in aromatic CD spectra suggest the changes in tertiary structure or the manner in which the secondary-structure elements interact (Ewbank & Creighton, 1991). The hydration apparently transformed segments of the secondary structure into β-turn-like components.

The results provide evidence for a quantitative relationship between perturbations of native β-pleated-sheet-like secondary and tertiary structure of scrapie amyloid, PrP27-30, and infectivity. Another interpretation could be that the observed changes in scrapie amyloid protein conformation paralleled the conformational changes of still undetected subfraction of scrapie amyloid protein or scrapie agent, responsible for scrapie transmission. However, this is largely a theoretical possibility and is difficult to prove or invalidate for technical reasons (Safar et al., 1990; Prusiner, 1992). It is possible that the β-pleated-sheet secondary and specific tertiary structure of PrP protein is solely responsible for its ability to propagate and amplify. The alternative explanation may be that the native conformation of PrP27-30 is critical for ligand binding, and only the entire complex can propagate, amplify, and form amyloid. This does not diminish the key role of the PrP27-30 protein structure, because any change in PrP27-30 conformation would result in changed binding of the ligand (Jaenicke, 1991) and in different biologic activity (infectivity). The biologic data on different "strains" of infectivity isolated from the animals with an identical primary sequence of PrP protein (Kimberlin et al., 1989; Hecker et al., 1992) may support the ligand concept (Weissmann, 1991) or alternative posttranslational modification (Safar et al., 1990; Prusiner, 1992). The least conventional explanation, the existence of multiple stable conformations of the same primary sequence under the same conditions able to specifically replicate itself from passage-to-passage, is difficult to incorporate into current models of protein folding thermodynamics (Creighton, 1990; Jaenicke, 1991).

Materials and methods

Reagents

FA (99%) was obtained from Sigma (St. Louis, Missouri). TFE, HFIP, TFA, and SDS were all spectroscopic or NMR grade from Aldrich (Milwaukee, Wisconsin). Other chemicals were reagent grade and of the highest purity commercially available.

Source of hamster PrP27-30

Golden Syrian hamsters LVG/LAK (Animal Production Area, Frederick Cancer Research Facility, Frederick, Maryland) were inoculated intracerebrally (i.c.) with 0.03 mL of a 10^{-2} dilution of hamster brain homogenate

infected with the seventh serial hamster passage of scrapie strain 263K. All animals were sacrificed during the advanced terminal stages of their illness, brains surgically removed under aseptic conditions, snap-frozen, and stored at −70 °C until used.

Bioassay

The infectivity assay was carried out in groups of eight weanling female golden Syrian hamsters LVG/LAK (Animal Production Area, Frederick Cancer Research Facility, Frederick, Maryland) inoculated i.c. with 0.03 mL of 10^{-2} or 10^{-3} dilution of the test sample in phosphate-buffered saline (PBS), pH 7.4. The clinical diagnosis of scrapie was confirmed by histopathologic evaluation of two randomly chosen hamster brains from each test sample. The titers were calculated from the incubation time as described (Prusiner, 1982), with some modifications. The original formula was fit by linear regression least-squares technique into a database with endpoint titers and incubation times obtained from 28 independent endpoint titrations on 417 female golden Syrian hamsters injected with the 263K strain of scrapie. The adapted formula differs in constants: $\log ID_{50}/mL = 16.571 - 7.495 \times \log(Ti - 40) - \log D$, where $\log ID_{50}/mL$ is the final titer in $\log_{10}$ of infectious units per milliliter of original sample, Ti is the incubation time in days, and $\log D$ is the dilution of the sample. The expected differences in intercept and slope from that published reflect the differences in experiments and probably also in scrapie strain (Prusiner et al., 1982). The correlation coefficient ($R = 0.8291$) between endpoint and incubation time-derived titers is highly significant ($P < 0.0001$).

Purification of hamster PrP^{Sc} and PrP27-30

The purification procedure of PrP^{Sc} is described in detail elsewhere (Safar et al., 1990). To cleave PrP^{Sc}, the protein was resuspended in PBS, pH 7.4, containing 2.3 M NaCl and 1% sarcosyl (w/v) to a final protein content of 1 mg/mL, and incubated with proteinase K (27 U/mg activity; Merck, Darmstadt, Germany) for 2 h at 37 °C in an enzyme/protein ratio of 1:40 (w/w). The reaction was stopped by adding 3 mM PMSF, 20 μg/mL aprotinin, and 10 μg/mL leupeptin; the sample was centrifuged at 13,000 × *g* (Beckman SW 55 rotor) for 15 min at 4 °C. The pellet was washed first in H_2O containing 0.1% sarcosyl, 2 μg/mL aprotinin, and 1 μg/mL leupeptin, then in TBS, pH 7.4, containing 2 μg/mL aprotinin and 1 μg/mL leupeptin, and then in TBS, pH 7.4, only.

Protein content

Protein content was calculated from the absorption coefficient ϵ_{205} (1 mg/mL; 1 cm) and absorbance at 205 nm as described (Scopes, 1974; Stevens, 1977; Safar et al., 1993). The standard solutions for ϵ_{205} determination were prepared from SE HPLC-purified PrP27-30 after amino acid determination as described (Safar et al., 1990). Absorbance spectra of the proteins in films were recorded from 200 to 320 nm with a Beckman spectrophotometer, model DU-68, in a 0.1-cm quartz Hellma square cell (also used in recording CD) at 23 °C against blanks with identical buffer composition. The signal was subtracted from the baseline spectra of an empty cell; the cell aperture and distance from the photomultiplier window were the same as for the solutions. The above procedure was not necessary for the samples run on a J-720 model, where the CD spectrum was recorded in parallel with an HT parameter and absorbance calculated by the software provided by the manufacturer (Jasco Inc., Easton, Maryland).

CD spectroscopy

The films were prepared as described previously (Safar et al., 1993), and the CD spectra are the averages of 4–10 scans with the baseline subtracted from corresponding blanks. Briefly, the PrP27-30 was sonicated five times at 5-s bursts at 50 W on ice using a BraunSonic 2000 and microprobe, and dialyzed for 24 h at 4 °C against three changes of H_2O. The samples containing 0.9 nmol of the protein in 150 μL of HPLC-grade H_2O were loaded inside the inner sinter ring of 0.01- or 0.001-cm-pathlength quartz sandwich cells (Hellma Cells Inc., Jamaica, New York). The films were dried under 20-mm Hg vacuum in a desiccator above KOH pellets for 24 h at 23 °C. The CD signal of the film remained stable at 4 °C for several days. Measurements were carried out with a Jasco spectropolarimeter, model J-500A/DP-501N or model J-720/PS2 (Jasco Inc.) and are expressed as mean residue ellipticity [θ] (Woody, 1985; Yang et al., 1986). The recording parameters were: bandwidth 1.0 nm, slit width auto, sensitivity 5–10 m°, response 4 s, scan speed 10 nm/min, and step resolution 0.025 nm. The mean residue weight calculated according to the DNA-deduced amino acid sequence starting at Gly 90 minus carboxyl-terminal domain is 109.5 for hamster PrP27-30. The data shown are representative spectra from three to five experiments.

High-temperature exposure and solvent replacement

The assembled sandwich cells with dry films of PrP27-30 were exposed to 23 °C, 60 °C, 100 °C, and 132 °C for 30 min in a sealed glass vial, and scanned at 23 °C after cooling as described (Safar et al., 1993). The temperature inside one vial was measured directly by a thermometer inserted through a silicon septum. When indicated, the films cast from protein in H_2O were dried and then overlaid with 100 μL of 99% FA, TFE, HFIP, or TFA, incubated for 30 min at 23 °C in a Parafilm-sealed and solvent-saturated petri dish, rapidly evaporated in Speed-Vac (Savant, Hicksville, New York) equipped with an

NaOH trap, and finally dried in a desiccator in a vacuum above KOH pellets for 24 h at 23 °C. Identical results were obtained when the protein was first dissolved in solvent and then cast in film and dried. The SDS/protein films were prepared from a PrP27-30 protein solubilized by 270× molar excess of SDS (SDS/protein molar ratio). The films were dried in a desiccator under vacuum above KOH pellets for 24 h at 23 °C.

The dry films were rehydrated in an H_2O-saturated atmosphere in a petri dish at 23 °C and CD spectra were recorded after 1 min, 30 min, 3 h, and 24 hr. Equivalent results were obtained when 0.001-cm-pathlength sandwich cell and films were directly overlaid with 15 μL of H_2O and scanned by CD. For bioassay, the rehydrated films were sonicated in PBS, pH 7.4, in a sonication bath before injection.

Deconvolution of CD spectra and analysis of secondary structure components

To analyze the solvent-induced perturbation of the secondary structure in the solid state and to extract common components, we used the CCA method developed by Perczel and Fasman (Perczel et al., 1991b). The set of the 12 CD spectra of PrP27-30 in the solid state after exposure to different solvents was used to construct a 46 × 12-data point matrix, which was analyzed by the CCA algorithm using IBM-compatible software made available by G.D. Fasman. CCA is a natural deconvolution algorithm that incorporates three constraints: (1) the sum of the secondary structure should be 100%; (2) each component would be a positive value (weight coefficient); and (3) each coefficient value for a given protein should be placed in a simplex of the P-dimensional Euclidean space with the smallest volume (volume minimization), where the value P is the number of the common components. The PrP27-30 matrix, instead of the original reference dataset (RDS) matrix (Perczel et al., 1991b), was deconvoluted on an IBM PS2 equipped with a numerical coprocessor. The deconvolution was repeated for 2–10 components and the standard deviation $\sigma(P)$ of each deconvolution was plotted against the number of components (P) to determine the inflection point. Assignment of each "pure" spectral component was done by comparing the CD spectrum with published or calculated standards. Using conformational weights (g) and pure component curves (p), the CD spectrum $[f(\lambda)]$ can be reconstructed from (n) components: $f(\lambda) = p_1 * g_1(\lambda) + p_2 * g_2(\lambda) + \ldots + p_n * g_n(\lambda)$.

SDS-PAGE, Western blots, and densitometry

The SDS-PAGE (formula T 12.5/C 3), silver-staining, and Western blotting of electrophoresed proteins are described elsewhere (Safar et al., 1990). The gels were scanned by a Shimadzu dual-wavelength flying-spot laser scanner model CS-9000, in a linear transmittance mode at 550 nm.

Acknowledgments

We are thankful for the CCA algorithm software, made available by Dr. G.D. Fasman through the courtesy of Jasco Inc. We thank Michael P. Sulima for excellent technical assistance, Devera G. Schoenberg for editing the manuscript, and Steve Ono and N. La-Donna Tavel for document production assistance.

References

Asher, D., Gibbs, C.J., & Gajdusek, D.C. (1986). Slow viral infections: Safe handling of the agents of subacute spongiform encephalopathies. In *Laboratory Safety: Principles and Practices* (Miller, B.M., Ed.), pp. 59–71. American Society for Microbiology, Washington, D.C.

Auer, H.E. (1973). Far-ultraviolet absorption and circular dichroism spectra of L-tryptophan and some derivatives. *J. Am. Chem. Soc. 95*, 3003–3011.

Barrow, C.J., Yasuda, A., Kenny, P.T.M., & Zagorski, M.G. (1992). Solution conformations and aggregational properties of synthetic amyloid β-peptides of Alzheimer's disease. *J. Mol. Biol. 225*, 1075–1093.

Brahms, S. & Brahms, J. (1980). Determination of protein secondary structure in solution by vacuum ultraviolet circular dichroism. *J. Mol. Biol. 138*, 149–178.

Brown, P., Liberski, P.P., Wolff, A., & Gajdusek, D.C. (1990a). Resistance of scrapie infectivity to steam autoclaving after formaldehyde fixation and limited survival after ashing at 360 degrees C: Practical and theoretical implications. *J. Infect. Dis. 161*, 467–472.

Brown, P., Wolff, A., & Gajdusek, D.C. (1990b). A simple and effective method for inactivating virus infectivity in formalin-fixed tissue samples from patients with Creutzfeldt-Jakob disease. *Neurology 40*, 887–890.

Caughey, B.W., Dong, A., Bhat, K.S., Ernst, D., Hayes, S.F., & Caughey, W.S. (1991). Secondary structure analysis of the scrapie-associated protein PrP 27-30 in water by infrared spectroscopy. *Biochemistry 30*, 7672–7680.

Creighton, T.E. (1990). Protein folding. *Biochem. J. 270*, 1–16.

Ewbank, J.J. & Creighton, T.E. (1991). The molten globule protein conformation probed by disulphide bonds. *Nature 350*, 518–520.

Gajdusek, D.C. (1988). Transmissible and nontransmissible dementias: Distinction between primary cause and pathogenetic mechanism in Alzheimer's disease and aging. *Mt. Sinai J. Med. 55*, 3–5.

Gasset, M., Baldwin, M.A., Fletterick, R.J., & Prusiner, S.B. (1993). Perturbation of the secondary structure of the scrapie prion protein under conditions that alter infectivity. *Proc. Natl. Acad. Sci. USA 90*, 1–5.

Greenfield, N. & Fasman, G.D. (1969). Computed circular dichroism spectra for the evaluation of protein conformation. *Biochemistry 8*, 4108–4116.

Hecker, R., Taraboulos, A., Scott, M., Pan, K.M., Yang, S.L., Torchia, M., Jendroska, K., Dearmond, S.J., & Prusiner, S.B. (1992). Replication of distinct scrapie prion isolates is region specific in brains of transgenic mice and hamsters. *Genes Dev. 6*, 1213–1228.

Hollosi, M., Urge, L., Perczel, A., Kajtar, J., Teplan, I., Otvos, L., Jr., & Fasman, G.D. (1992). Metal ion-induced conformational changes of phosphorylated fragments of human neurofilament (NF-M) protein. *J. Mol. Biol. 223*, 673–682.

Jaenicke, R. (1987). Folding and association of proteins. *Prog. Biophys. Mol. Biol. 49*, 117–237.

Jaenicke, R. (1991). Protein folding: Local structures, domains, subunits, and assemblies. *Biochemistry 30*, 3147–3161.

Jaenicke, R. & Rudolph, R. (1986). Refolding and association of oligomeric proteins. *Methods Enzymol. 131*, 218–250.

Kimberlin, R.H., Walker, C.A., & Fraser, H. (1989). The genomic identity of different strains of mouse scrapie is expressed in hamsters and preserved on reisolation in mice. *J. Gen. Virol. 70*, 2017–2025.

Kugo, K., Okuno, M., Kitayama, K., Kitaura, T., Nishino, J., Ikuta,

N., Nishio, E., & Iwatsuki, M. (1992). Fourier transform IR attenuated total reflectance study on the secondary structure of poly(γ-methyl L-glutamate) surfaces treated with formic acid. *Biopolymers 32*, 197-207.

Matthews, C.R. & Crisanti, M.M. (1981). Urea-induced unfolding of the α subunit of tryptophan synthase: Evidence for a multistate process. *Biochemistry 20*, 784-792.

Miick, S.M., Martinez, G.V., Fiori, W.R., Todd, A.P., & Millhauser, G.L. (1992). Short alanine-based peptides may form 3_{10}-helices and not α-helices in aqueous solution. *Nature 359*, 653-655.

Nakajima, A., Fujiwara, T., Hayashi, T., & Kaji, K. (1973). Occurrence of β-chain conformation in poly-γ-methyl glutamate membranes. *Biopolymers 12*, 2681-2690.

Park, K., Flyn, G.C., Rothman, J.E., & Fasman, G.D. (1993). Conformational change of chaperone Hsc70 upon binding to a decapeptide: A circular dichroism study. *Protein Sci. 2*, 325-330.

Park, K., Perczel, A., & Fasman, G. (1992). Differentiation between transmembrane helices and peripheral helices by the deconvolution of circular dichroism spectra of membrane protein. *Protein Sci. 1*, 1032-1049.

Perczel, A. & Fasman, G.D. (1992). Quantitative analysis of cyclic beta-turn models. *Protein Sci. 1*, 378-395.

Perczel, A., Hollosi, M., Foxman, B.M., & Fasman, G.D. (1991a). Conformational analysis of pseudocyclic hexapeptides based on quantitative circular dichroism (CD), NOE, and X-ray data—The pure CD spectra of type-I and type-II beta-turns. *J. Am. Chem. Soc. 113*, 9772-9784.

Perczel, A., Hollosi, M., Tusnady, G., & Fasman, G.D. (1991b). Convex constraint analysis: A natural deconvolution of circular dichroism curves of proteins. *Protein Eng. 4*, 669-679.

Prusiner, S.B. (1982). Novel proteinaceous infectious particle causes scrapie. *Science 216*, 136-144.

Prusiner, S.B. (1992). Chemistry and biology of prions. *Biochemistry 31*, 12277-12288.

Prusiner, S.B., Cochran, S.P., Groth, D.F., Downey, D.E., Bowman, K.A., & Martinez, H.M. (1982). Measurement of the scrapie agent using an incubation time interval assay. *Ann. Neurol. 11*, 353-358.

Prusiner, S.B., Groth, D., Serban, A., Stahl, N., & Gabizon, R. (1993). Attempts to restore scrapie prion infectivity after exposure to protein denaturants. *Proc. Natl. Acad. Sci. USA 90*, 2793-2797.

Prusiner, S.B., McKinley, M.P., Bowman, K.A., Bolton, D.C., Bendheim, P.E., Groth, D.F., & Glenner, G.G. (1983). Scrapie prions aggregate to form amyloid-like birefringent rods. *Cell 35*, 349-358.

Rohwer, R.G. (1984). Scrapie shows a virus-like sensitivity to heat inactivation. *Science 223*, 600-602.

Safar, J., Roller, P.P., Ruben, G.C., Gajdusek, D.C., & Gibbs, C.J. (1993). Secondary structure of proteins associated in thin films. *Biopolymers 33*, 1461-1476.

Safar, J., Wang, W., Padgett, M.P., Ceroni, M., Piccardo, P., Zopf, D., Gajdusek, D.C., & Gibbs, C.J., Jr. (1990). Molecular mass, biochemical composition, and physicochemical behavior of the infectious form of the scrapie precursor protein monomer. *Proc. Natl. Acad. Sci. USA 87*, 6373-6377.

Schulz, G.E. & Schirmer, R.H. (1979). *Principles of Protein Structure*. Springer-Verlag, New York, Berlin, Heidelberg, Tokyo.

Scopes, R.K. (1974). Measurement of protein by spectrophotometry at 205 nm. *Anal. Biochem. 59*, 277-282.

Stevens, E.S. (1977). Far (vacuum) ultraviolet circular dichroism. *Methods Enzymol. 49*, 214-221.

Stevens, L., Townend, R., Timasheff, S.N., Fasman, G.D., & Potter, J. (1968). The circular dichroism of polypeptide films. *Biochemistry 7*, 3717-3720.

Weissmann, C. (1991). A 'unified theory' of prion propagation. *Nature 352*, 679-683.

Woody, R.W. (1985). Circular dichroism of peptides. In *Conformation in Biology and Drug Design* (Hruby, V.J., Ed.), pp. 15-114. Academic Press, New York.

Yang, J.T., Wu, C.C., & Martinez, H.M. (1986). Calculation of protein conformation from circular dichroism. *Methods Enzymol. 130*, 208-269.